Attenuation of neutron and photon-induced irradiation damage in pressurized water reactor pressure vessels

Shengli Chen, David Bernard, Patrick Blaise

Version of Record: https://www.sciencedirect.com/science/article/pii/S0306454920302991
Manuscript_6fd6587353ca673b41a0e9ad5dd35046

Attenuation of neutron and photon-induced irradiation damage in pressurized water reactor pressure vessels

Shengli Chen[1,3,*], David Bernard[1], Patrick Blaise[2]

[1] CEA, DES, IRESNE, DER, SPRC, LEPh, 13108 Saint Paul Les Durance, France

[2] CEA, DES, IRESNE, DER, SPESI, 13108 Saint Paul Les Durance, France

[3] Université Grenoble Alpes, I-MEP2, 38402 Saint Martin d'Hères, France

[*] Corresponding author: shengli.chen@cea.fr

Abstract

The present work investigates the attenuation of neutron and photon-induced irradiation damage in a Pressurized Water Reactor (PWR)-like mock-up Reactor Pressure Vessel (RPV) using Tripoli-4® Monte Carlo simulations with a particular emphasis on the presence of a thick stainless steel heavy reflector between the core and RPV. Results show that the photon-induced damage is well described by the exponential law. The neutron-induced damage attenuates quicker than the exponential form near the outer surface of RPV. Nevertheless, an exponential form can represent the attenuation of neutron-induced damage within 5% discrepancy for penetration < 17 cm in a typical 22 cm thick RPV and within 20% in the outermost 3 cm. The exponential form with an additional negative term fits the attenuation of neutron-induced damage in RPV as the negative term considers the "leakage" of neutron near the outer surface. It is observed that the presence of a Gen III-like representative heavy reflector reduces the estimated neutron-induced damage by a factor of 2. On the other hand, this paper verifies that the neutron flux with energies above 0.5 MeV ($\phi_{>0.5}$) is more representative of the displacement damage attenuation than the flux above 0, 0.1, and 1 MeV in RPVs. The damage rate is approximatively equal to $K\phi_{>0.5}$ with $K = 9.5 \times 10^{-22}$ DPA/(n · cm^{-2}) in PWR RPVs.

Keywords: Displacement per Atom, Reactor Pressure Vessel, Heavy reflector, PERLE experiment, Attenuation, Neutron and Photon, Monte Carlo simulation

1. Introduction

The irradiation-induced damage in the Reactor Pressure Vessel (RPV) is one of the most important issues for commercial Pressurized Water Reactors (PWRs). The number of Displacement per Atom (DPA) is widely used to quantify the irradiation damage of materials. Due to the slowing down and absorption of neutrons in RPV, the DPA attenuates with increasing penetration in RPV. Stoller and Greenwood [1] investigated the neutron-induced DPA in different penetrations in RPV using both the standard Norgett-Robinson-Torrens (NRT) formula [2] and Molecular Dynamics (MD) simulations. Carew and Hu [3] studied the radial and axial dependence of neutron-induced DPA in RPV. Remec [4] investigated the DPA attenuation in RPVs with

different thicknesses thermal shield and RPV. Ref. [3] points out that a simple exponential form cannot fit the shape of attenuation of neutron-induced DPA in stainless steel (SS) RPVs, whereas our previous paper [5] shows that the exponential form is quite suitable to describe the attenuation of neutron-induced DPA rates in the SS heavy reflector. Since the neutron and photon (called also as gamma-ray) spectra in a RPV are quite different to those in a SS heavy reflector (details are presented in Section 3), this paper investigates the attenuation of neutron and photon-induced DPA in RPVs with and without a 22 cm thick SS heavy reflector surrounding the core, using Tripoli-4® [6] Monte Carlo simulation. The methods are summarized in Section 2. The results and discussion are presented in Sections 3.2 and 3.3.

On the other hand, since the measurement of fast neutron fluence is much easier than the measurement of accumulated DPA, the fast neutron fluence is traditionally used to correlate DPA. In general, the neutron fluence above 1 MeV is considered for experimental neutron irradiation damage measurement [7]. However, Refs. [1], [3] show that the attenuation of DPA is different from the recommended formula of the US Nuclear Regulatory Commission (NRC) regulatory guide 1.99 revision 2 [8], based on neutron fluence above 1 MeV [8]. Our recent work [5] points out that the neutron fluence above 0.5 MeV is quite representative of DPA in the SS heavy reflector from the point of view of attenuation. Moreover, the 0.5 MeV threshold is the Eastern European Standard [7]. Therefore, the present work compares the attenuations of DPA and neutron fluence with different threshold energies in Section 3.4. An empirical formula for correlating DPA with neutron fluence above 0.5 MeV is also deduced in Section 3.4.

2. Description of the models

2.1 Monte Carlo simulations

In the European Gen III design, the core is surrounded by a heavy reflector with 8 cm to 30 cm thickness [9]. The PERLE experiment [10], [11] was designed for studying neutron properties in a representative Gen III thick stainless steel reflector. As the present work focuses on the verification and validation of the methodology, the PERLE-based PWR-like mock-ups are used as purely numerical benchmarks, in order to economize the computation burden of Monte Carlo simulations. A typical 22 cm thick RPV (not present in the experiment) is added for studying the neutron and photon-induced irradiation damage. The typical thermal peaks of neutron spectra in the RPV are observed in the RPV of such a simplified PWR mock-up (shown in Section 3). The 1/4 configuration of the PERLE experiment with an additional RPV is shown in Figure 1(a).

In a typical Gen II PWR, the reactor core is enclosed by a ~3 cm SS baffle. For the sake of comparison, we use the same geometry of the PERLE core but a different reflector for a typical PWR. Since the baffle is about 10 times thinner than the heavy reflector, we use for an example a case in which the core is directly surrounded by the moderator without a reflector (shown in Figure 1(b)).

In addition, the primary concrete and the 30 cm air between the RPV and the

primary concrete are considered to simulate the neutron and photon reactions outside the outer surface of RPV. All Tripoli-4.10 Monte Carlo simulations are based on the JEFF-3.1.1 evaluated pointwise nuclear data library [12]. The accuracy of Tripoli-4 simulations of the PERLE core and heavy reflector with JEFF-3.1.1 was validated against experimental measurements on reactivity [5], [11], [13], pin-by-pin power distribution [11], neutron and photon doses in the SS heavy reflector [11], [13]. The neutron and photon spectra used for calculating DPA rates in the RPV are the volume-averages in the hollow cylinders for z-axis from the bottom to the top of fuel pins. The thicknesses of these hollow cylinders are respectively 1 cm for the innermost 4 ones, 2 cm for the middle 3 ones, and 3 cm for the outermost 4 ones for optimizing the computation burden and the statistical uncertainties from stochastic simulations.

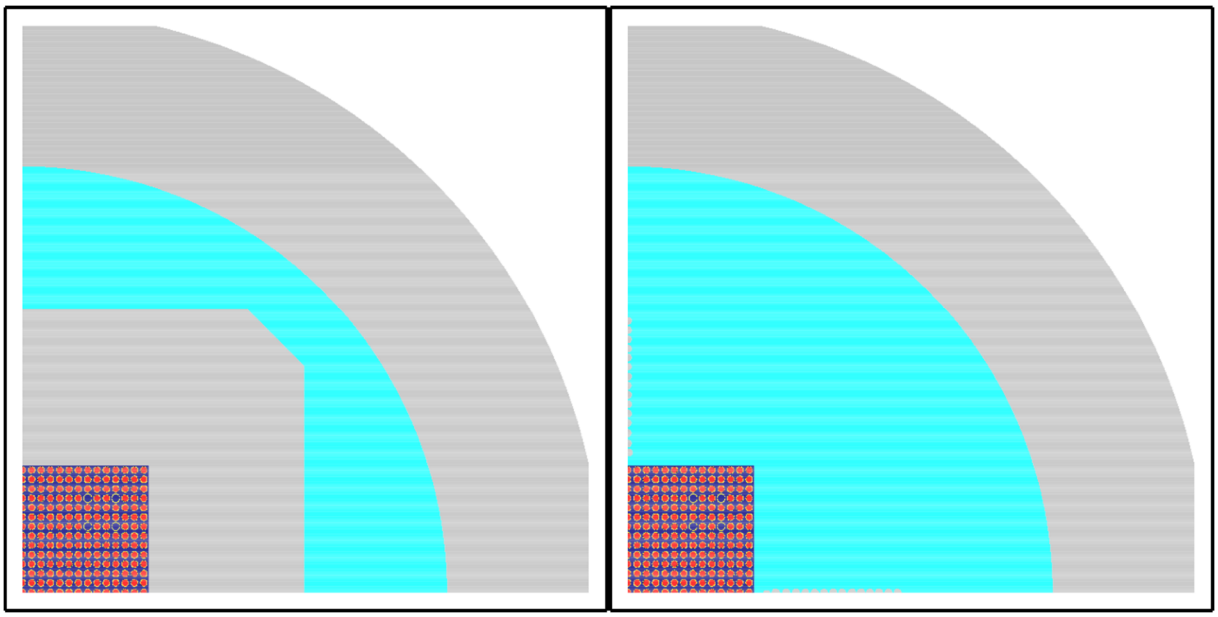

Figure 1. Configuration of the 1/4 geometry of the PERLE experiment by adding a 22 cm thick RPV with (left) and without the SS heavy reflector (right). The primary concrete and the enclosed air are included but not shown in this figure.

2.2 Attenuation of DPA

The present work focuses on studying the DPA. However, it should be noted that DPA is only a quantity used to estimate the irradiation damage: DPA is *not* equivalent to damage. Because the attenuations of DPA using both MD simulations and NRT formula are almost the same [14], the present work directly uses the current international standard NRT metric. As explained in Ref. [5], the DPA rates presented in this paper are calculated by folding the neutron and photon flux spectra from Tripoli-4.10 simulations with the corresponding neutron and photon-induced damage cross sections. By analogy to the attenuation of flux density in a 1-D approximation, our previous work [5] proposed a simple formula for describing the neutron-induced DPA rate versus the penetration in steel reflector as:

$$DPA_n(x) = DPA_{n0} e^{-\Sigma_n^{DPA} x}. \quad (1)$$

where x represents the penetration in material, Σ_n^{DPA} and DPA_{n0} are free parameters

that can be deduced from computation data fitting.

It should be noted that Ref. [3] points out that the neutron-induced DPA in a RPV should require an additional term of the form:

$$DPA_n(x) = Ae^{-Bx} + C \quad (2)$$

where A, B, and C are determined by numerical fitting. An intuitive explanation of the additional parameter is due to the leakage of neutrons at the outer surface of RPV. Therefore, C should be negative. More discussion on this formula is found in Section 3.3. For simplification, the fittings of the neutron-induced DPA using Eqs. (1) and (2) are simply noted by neutron (1) and neutron (2) hereinafter. The number 1 or 2 corresponds to the number of free parameters for the normalization: 1 in Eq. (1) (i.e. DPA_{n0}) and 2 in Eq. (2) (i.e. A and C). It is noted that the attenuation coefficient B in Eq. (2) obtained from the least square fitting is numerically different from the value of Σ_n^{DPA} in Eq. (1). Therefore, the difference between the fittings from Eqs. (1) and (2) is not simply equal to the numerical value of C from fitting.

In the heavy reflector, due to the important albedo of thermal neutrons from the external moderator, the thermal neutron radiative capture reaction rate is an important source of photon production [5]. In the vicinity of the RPV outer surface, because there are only negligible backscattered thermal neutrons (as illustrated in Figure 2), the photon-induced DPA can be simplified as:

$$DPA_\gamma(x) = DPA_{\gamma 0} e^{-\Sigma_\gamma^{DPA} x} \quad (3)$$

where Σ_γ^{DPA} and $DPA_{\gamma 0}$ are free parameters that can be deduced from fitting.

3. Results and discussion

3.1 Attenuation of neutron flux and photon flux

Figure 2 shows the neutron spectra at different penetrations in the RPV with a 22 cm SS heavy reflector. The typical thermal peaks of neutron spectra close to the inner surface of a PWR RPV are found in Figure 2. We remark that all neutron and photon spectra shown in this paper are renormalized by a 40 W thermal power, which is the power of the PERLE experiment. As explained in Ref. [5], the dips of neutron spectra are induced by resonant reactions. Owing to the slowing down and absorption of neutrons in the RPV, the neutron flux decreases with the penetration. The increase of thermal neutrons near the external surface of RPV (e.g. comparing neutron flux at 14.5 and 20.5 cm penetrations in Figure 2) is due to the slowing down and "reflection" by the primary concrete (i.e. the biological shield wall) and the enclosed air. For comparison, Figure 11 in the Appendix shows the ratios of neutron spectra computed without considering the primary concrete nor the air between the RPV and the concrete (i.e. leakage boundary condition at the outer surface of RPV) to the neutron flux spectra shown in Figure 2.

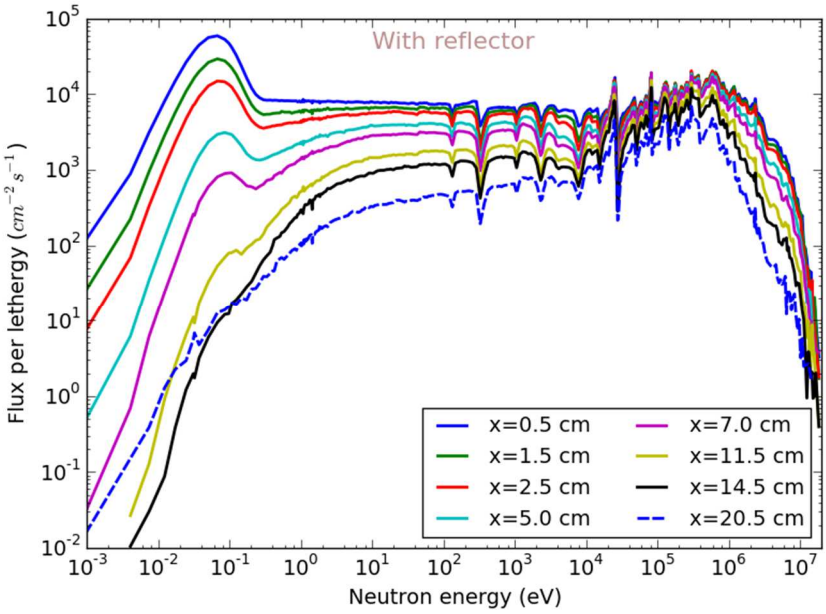

Figure 2. Neutron spectra at different penetrations in the RPV with a 22 cm SS heavy reflector. The Monte Carlo statistical uncertainties of neutron flux are within 3% for most groups and within 0.5% for total flux.

Comparing the neutron flux spectra in the RPV shown in Figure 2 with those in the SS heavy reflector shown in Ref. [5], one can find much higher proportions of thermal neutron in RPV because of the slowing down by the moderator surrounding the reflector. As a consequence, most conclusions shown in Ref. [5] for a SS heavy reflector are not necessarily the same as those in the RPV. Similarly, it is also the case for photon-induced DPA if one compares the photon spectra in RPV shown in this paper and those in the SS heavy reflector shown in Ref. [5]. Therefore, the present work focuses on the properties of DPA in the RPV.

The prompt photon spectra at different penetrations are shown in Figure 3. The methods for simulating electron and photon transport in Tripoli-4 are explained in Ref. [15]. The peaks of the photon spectra in the RPV respectively correspond to: electron-positron annihilation (0.511 MeV), inelastic scattering of ^{56}Fe (0.847 MeV), and neutron radiative capture reactions of ^{1}H (2.22 MeV), ^{55}Mn (7.27 MeV), ^{58}Ni (9.00 MeV), and ^{53}Cr (9.72 MeV).

From Figure 3, it is observed that the photon flux above the displacement threshold 0.63 MeV [16] and below 10 MeV follows the exponential law of attenuation well. The photon flux with energies higher than 10 MeV is more than 3 orders of magnitude lower than those at several MeV. Since the photon-induced DPA cross section at 15 MeV is only 7 times larger than that at 5 MeV [5], [16], the photons with energies above 10 MeV have a quite limited contribution to photon-induced atomic displacement. Therefore, the attenuation of photon-induced atomic displacement in the RPV should have an exponential form as given in Eq. (3).

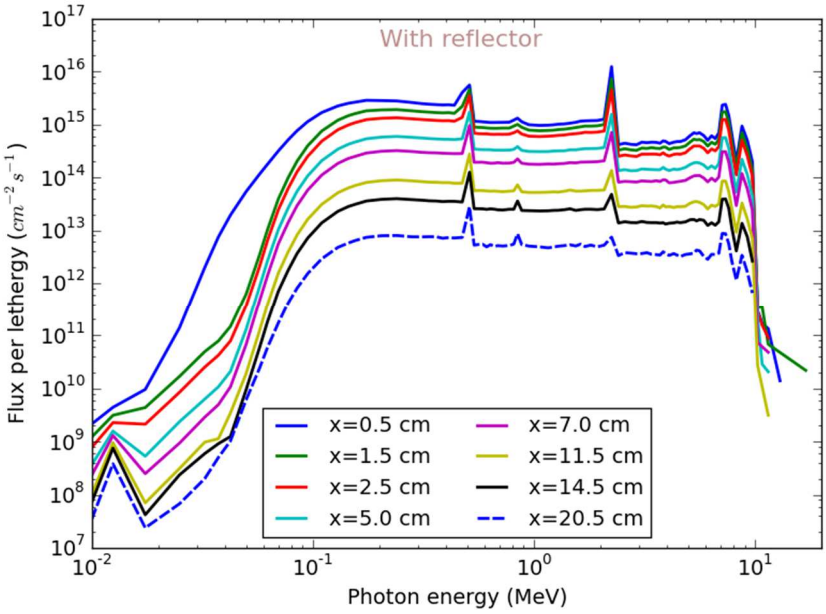

Figure 3. Photon spectra at different penetrations in the RPV.

The case with a 22 cm thick heavy reflector and primary concrete and the enclosed 30 cm air is referred to as the reference case hereinafter. The ratios of neutron spectra and photon spectra in the case of no reflector to those of the reference case are respectively illustrated in Figure 4. Compared with the case with a SS heavy reflector, the neutron flux in the RPV without a reflector has a larger proportion of fast neutrons. For photon flux, the attenuation also follows the exponential law well above the 0.63 MeV threshold for atomic displacements [16]. More photons with energies above 10 MeV are found without a SS reflector. However, as previously explained, due to the quite negligible quantity as shown in Figure 4, the photons with energies above 10 MeV are negligible for the contribution to total damage.

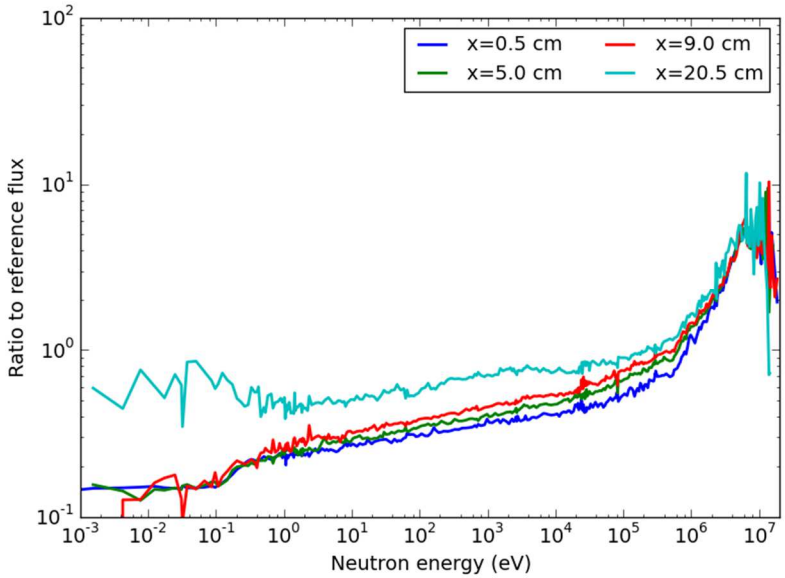

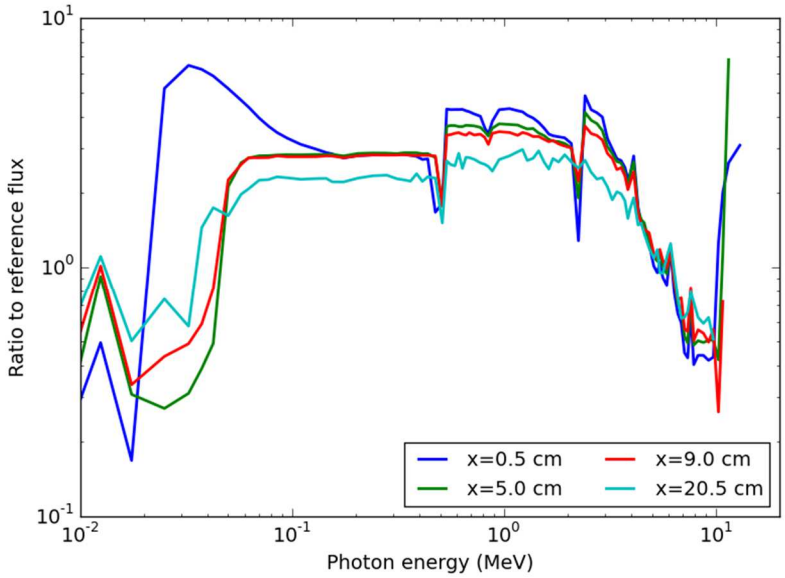

Figure 4. Ratio of neutron (upper) and photon (lower) spectra at different penetrations in the RPV without a reflector to the reference case

3.2 Attenuation of DPA rate

In the present work, the total neutron and photon-induced DPA rates are calculated using the neutron and photon spectra from Tripoli-4.10 Monte Carlo simulations and the corresponding DPA cross sections (the self-shielding correction on multigroup DPA cross section [17] is not considered here). The total neutron-induced damage cross sections calculated by NJOY-2016 [18] are used in the present work. The total photon-induced DPA cross sections are from our previous work [16]. In order to show the results more comparable to commercial reactors, all the DPA rates shown in this paper are renormalized according to the neutron flux density of a 4500 MWth Gen III commercial reactor as explained in Ref. [5].

The total neutron and photon-induced irradiation damage in the RPV are illustrated in Figure 5 with scattered points. The results without a reflector are shown in Figure 6. The 1σ uncertainties of DPA rates due to statistical uncertainties from Monte Carlo simulation are respectively within 3% and 5% for neutron and photon-induced DPA rates (without considering the correlation matrix between flux at different energy groups, i.e. the direct sum of uncertainties of DPA rates in different groups) whether with or without a heavy reflector. The neutron-induced DPA rates are about 100 times larger than the photon-induced ones in the RPVs, whereas the factor is about 5000 in the SS heavy reflector [5]. This is a consequence of a much more efficient attenuation of neutrons than photons in the moderator, as explained by Alexander and Rehn [19]. Even though the photon-induced damage is negligible in a PWR reflector and RPV, it is noted that it is comparable with neutron-induced DPA in a Boiling Water Reactor (BWR) RPV [19], [20] and in the High Flux Isotope Reactor (HFIR) surveillance [21].

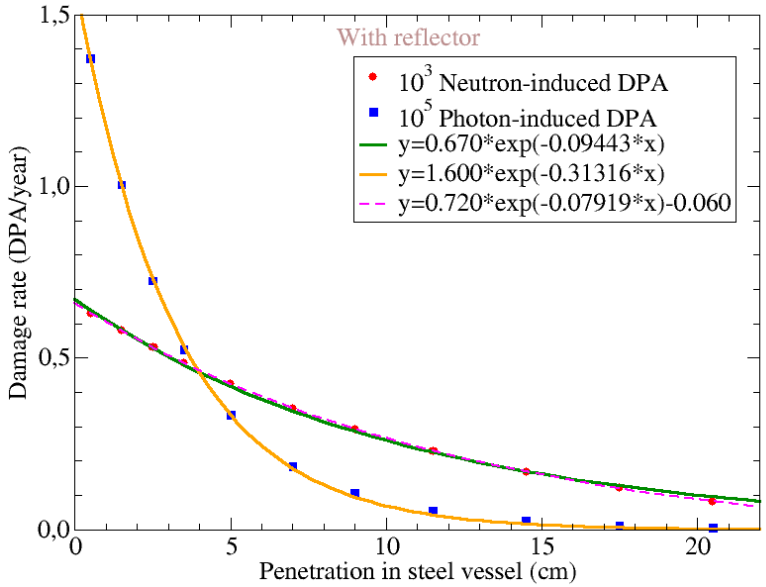

Figure 5. Attenuation of DPA rates in the simulated RPV of the PERLE experiment (i.e. with a SS heavy reflector)

The curves illustrated in Figure 5 and Figure 6 represent non-linear curve fittings for the cases with and without a heavy reflector. The corresponding analytical expressions are given in the corresponding legends. For photon-induced atomic displacement rate (in DPA/year) versus the penetration (in cm) in the RPV, the analytical expression

$$DPA_{\gamma}(x) = 1.600 \times 10^{-5} e^{-0.31316x} \tag{4}$$

is determined in the case of a 22 cm heavy reflector (Figure 5) and the formula

$$DPA_{\gamma}(x) = 1.536 \times 10^{-5} e^{-0.28739x} \tag{5}$$

is obtained for the case without a reflector (Figure 6). The corresponding coefficients of determination (R^2) and the chi-square goodness of fit (χ^2) are given in Table 1. Both the graphical illustrations in Figure 5 and Figure 6 and the quantitative summaries in Table 1 show that the exponential formula (3) gives a quite good description of the attenuation of photon-induced damage in RPVs. The non-linear curve fittings also show that the photon-induced irradiation damage at the inner surface of a RPV is similar both with and without a SS reflector.

Table 1. Goodness of non-linear curve fitting of the attenuation of damage rates

	With reflector			Without reflector		
	Photon	Neutron (1)	Neutron (2)	Photon	Neutron (1)	Neutron (2)
R^2	0.99992	0.99931	0.99997	0.99997	0.99911	0.99974
χ^2	0.00053	0.00055	0.00002	0.00698	0.02110	0.01091

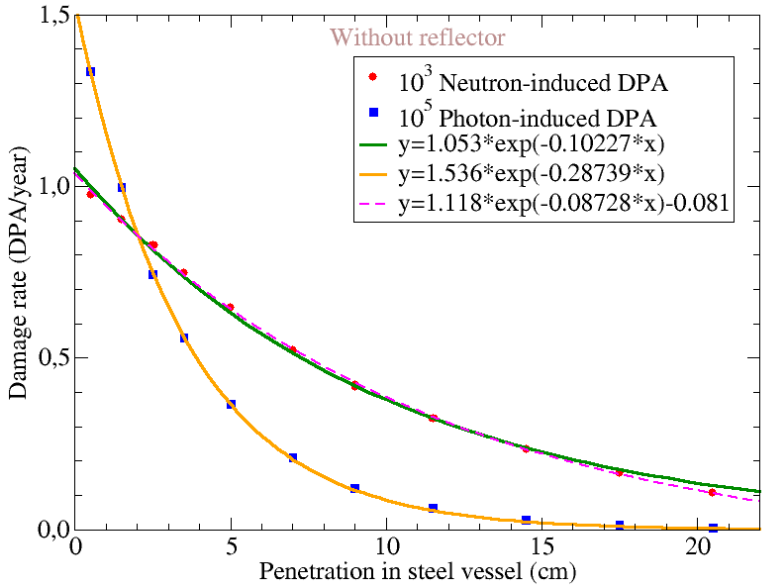

Figure 6. Attenuation of DPA rates in the simulated RPV of the PERLE experiment without a reflector

For neutron-induced damage shown in Figure 5 (i.e. with a SS heavy reflector) and Figure 6 (i.e. without a SS heavy reflector), the exponential form (i.e. Eq. (1)) is not sufficient to describe the DPA rate for penetration x > 17 cm. If one considers only the region where x < 17 cm, the fitted exponential forms

$$DPA_n(x) = 0.670 \times 10^{-3} e^{-0.09443x} \quad (6)$$

and

$$DPA_n(x) = 1.053 \times 10^{-3} e^{-0.10227x} \quad (7)$$

with x in cm and DPA_n in DPA/year, are suitable for predicting the attenuation of neutron-induced damage in RPVs with and without a heavy reflector, respectively. In the whole region of a RPV, Eq. (2) gives an accurate description of the attenuation of neutron-induced damage (in DPA/year):

$$DPA_n(x) = (0.720e^{-0.07919x} - 0.060) \times 10^{-3} \quad (8)$$

for the case of a 22 cm heavy reflector and

$$DPA_n(x) = (1.118e^{-0.08728x} - 0.081) \times 10^{-3} \quad (9)$$

without a reflector. The goodness of fitting for neutron-induced damage with Eqs. (1) and (2) are also summarized in Table 1.

It is found that the presence of a 22 cm SS heavy reflector reduces the neutron-induced damage by a factor close to 2. Since the case without reflector directly replaces the SS heavy reflector by moderator, the distance between the core and RPV of this case is larger than the realistic case. If a smaller and more realistic distance between the core and RPV is considered, the neutron-induced DPA rates are larger than the ones obtained by directly replacing the SS reflector by the moderator. Consequently, the reduction of the neutron-induced damage by the presence of the 22 cm SS heavy reflector should be larger than a factor of 2. The conclusion on the total damage rate is the same as the neutron-induced one because the photon-induced damage is smaller than 3% of the neutron-induced damage. The reduction of irradiation damage in RPV owing to the

presence of a SS heavy reflector is thus verified for Gen III reactors.

3.3 Further discussion on the attenuation of DPA rate

Figure 5 and Figure 6 point out that the exponential form is not sufficient to deal with the attenuation of neutron-induced damage at a penetration in a RPV larger than 17 cm. In fact, the simple reasoning (as given in Ref. [5]) that the attenuation of irradiation damage follows an exponential law is based on the number of neutrons passing through the surface. However, a neutron passing through a surface is not equivalent to neutron reacting at this surface. As the 2D example illustrated in Figure 7, except for the neutrons having collisions at both x and $x+dx$ (blue paths) or being absorbed in $[x, x+dx]$ (orange paths), the neutrons having reactions at penetration $x+dx$ can be from multiple scatterings of neutrons passing through x but without reaction at x (red paths). Similarly, the neutrons at x can be scattered to a penetration larger than $x+dx$ (green paths). In the intermediate region of a specific material, the balance between the red paths and green paths shown in Figure 7 leads to an exponential form of the attenuation of neutron flux and DPA. However, near the surfaces of the material, this balance is not guaranteed.

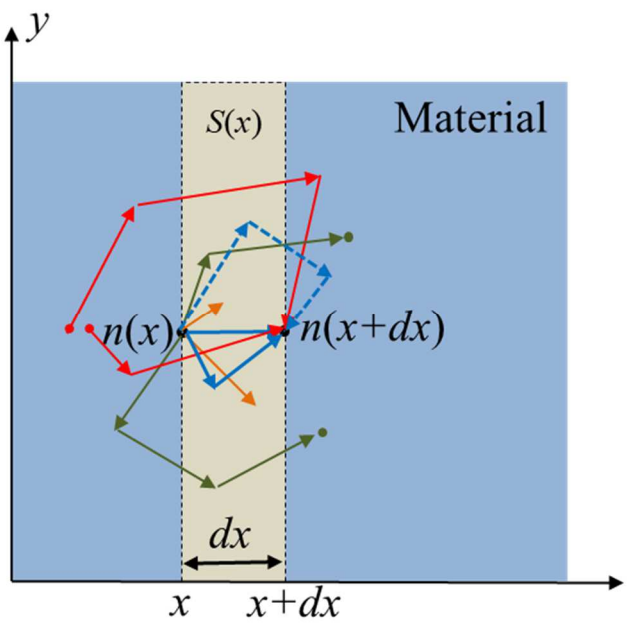

Figure 7. Schematic of neutron transport in 2D geometry

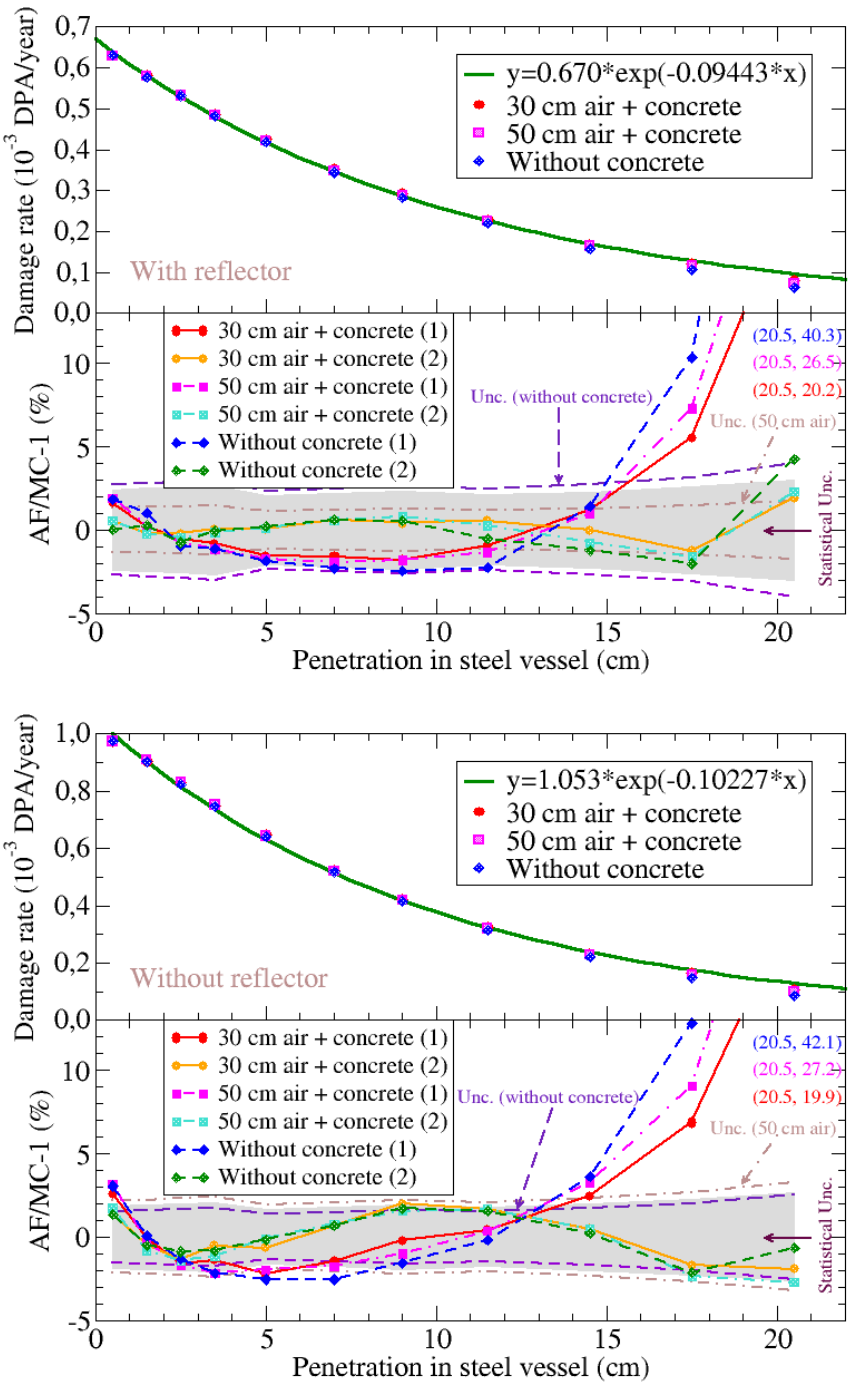

Figure 8. Attenuation of neutron-induced damage in the RPV with (upper) and without (lower) a SS reflector and the primary concrete. The lower subplots illustrate the differences between the Analytical Fitting (AF) of each case (shown in Figure 5, Figure 6, Figure 12, and Figure 13) and the Monte Carlo (MC)-based results. The large AF/MC discrepancies at 20.5 cm penetration are numerically pointed out in the figures. The directly summed statistical uncertainties (1σ) from MC simulations are shown for comparison.

Near the outer surface of RPV, the attenuation should be faster than the exponential form if there is no material surrounding the RPV (the sources from red paths and dashed

blue paths illustrated in Figure 7 are reduced). The air/concrete can reflect the neutrons going out of the RPV (comparing Figure 2 and Figure 11), the attenuation of damage rate near the outer surface of RPV without the surrounding air/concrete is thus higher than that with the surrounding air/concrete. In order to quantitatively show the effect at the periphery of RPV, Figure 8 compares the Monte Carlo simulation-based DPA rates with exponential analytical fitting. Figure 8 shows also the discrepancy between calculations and fittings with an additional negative term, noted as neutron (2) (notation defined in Section 2.2).

Upper subplots in Figure 8 show together the neutron-induced damage with 50 cm air + concrete and without air/concrete. The analytical fittings of neutron and photon-induced DPA rates without air/concrete (with 50 cm air between the RPV and concrete, resp.) surrounding are shown in Figure 12 (Figure 13 resp.) in the Appendix. The analytical exponential formulae given in Figure 5 and Figure 6 (i.e. from the standard simulations) are also included for intuitive comparison. Lower subplots in Figure 8 illustrate the differences between the calculated DPA rates and the analytical fittings (shown in Figure 5, Figure 6, Figure 12, and Figure 13). In other words, the differences shown in lower subplots in Figure 8 are individually deduced from the fittings and calculated points shown in Figure 5, Figure 6, Figure 12, and Figure 13.

In fact, the air between the RPV and the primary concrete have a negative contribution to DPA near the outer surface of RPV due to a lower backscattering-to-absorption ratio in the air and concrete than that in the RPV SS. This can be verified by comparing the results with 30 cm and 50 cm air shown in Figure 8 and comparing the results with different thicknesses RPVs investigated by Remec [4]. Therefore, it is emphasized that the primary concrete and the air between the RPV and the concrete should be considered in neutronic calculations for studying neutron-induced irradiation damage near the outer surface of RPV. Comparing the discrepancies to the corresponding exponential fittings for the three cases (30 cm air + concrete, 50 cm air + concrete, and without concrete), one can deduce that the attenuation of neutron-induced damage should be closer to an exponential form if the SS thermal insulation barrier [22] is used.

On the contrary, close to the inner surface of a RPV, the attenuation is slower than the exponential law because the source from red paths shown in Figure 7 is enhanced. Consequently, the damage rates near the inner surface are slightly below the exponential curves. Nevertheless, Figure 8 verifies that the exponential law can describe the neutron-induced damage at x = 0.5 cm (simulated in the volume determined by x = 0 and x = 1 cm) within 2% (3% without air/concrete) overestimation for the two cases (i.e. with a 22 cm heavy reflector and without a reflector).

In general, Figure 8 shows that the exponential law can well describe the attenuation of neutron-induced damage until 17 cm penetration within 5% discrepancy in a typical 22 cm thick RPV. For penetration x > 17 cm, the fitted exponential formula overestimates the damage due to the strong "leakage" of neutrons near the outer surface. For the outermost 3 cm thick volume, this overestimation reaches 20% (40% if air/concrete is not considered) whether with or without the heavy reflector. However, this overestimation is not very important because of the relatively small irradiation

damage. Eq. (2) with $C < 0$ (due to the "leakage") is shown able to fit the attenuation of neutron-induced DPA with the discrepancy included in the statistical uncertainty.

3.4 Comparison of total DPA with neutron flux

Our previous work shows that neutron flux above 0.5 MeV is representative of DPA in the SS heavy reflector [5]. However, because the neutron flux spectra in RPV are quite different from those in SS heavy reflector (c.f. Section 3), this conclusion cannot be directly generalized for a RPV. This subsection thus studies the representativity of neutron flux of total DPA in RPVs.

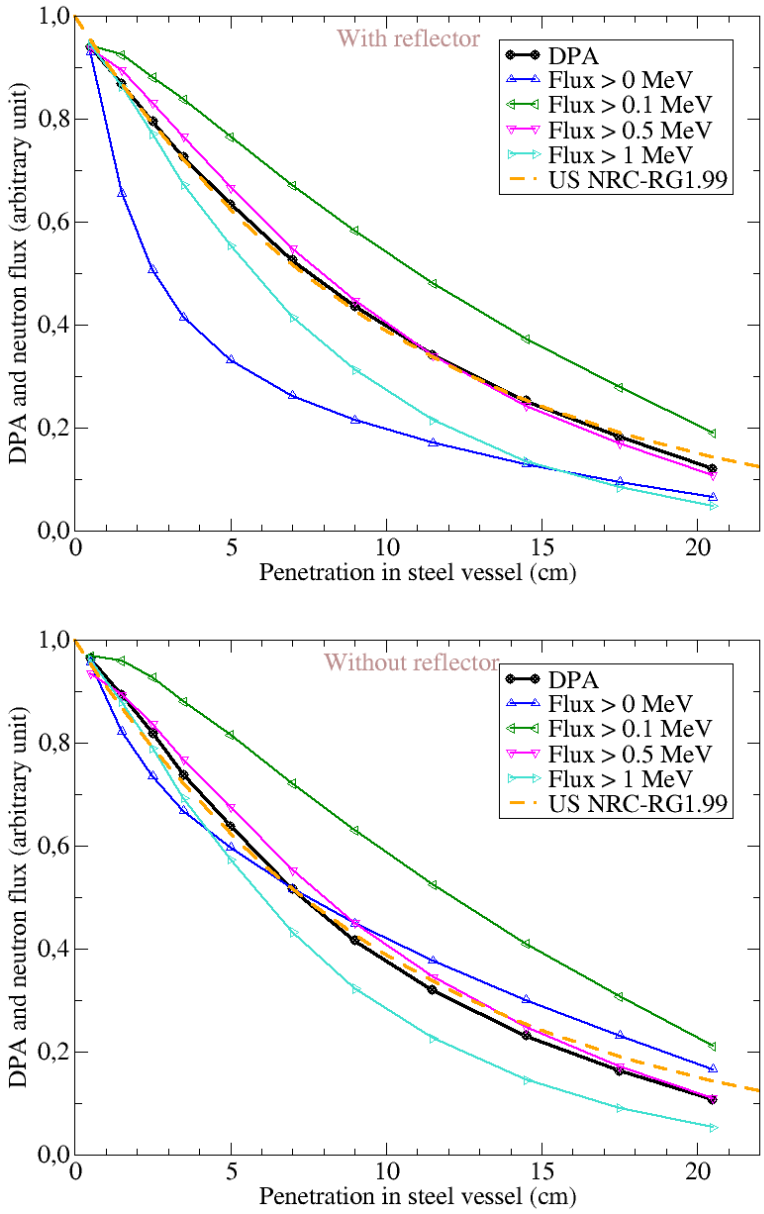

Figure 9. DPA rates and neutron flux in RPV from Monte Carlo simulations with (upper) and without (lower) reflector by arbitrary renormalizations. The different normalizations are used only for an intuitive comparison of the attenuations.

Figure 9 compares the attenuation of total DPA rates and neutron flux in RPVs. The data shown in Figure 9 are renormalized by arbitrary values for the sake of intuitive

comparison. As explained in Ref. [5], the attenuation of DPA rates based on the NRT metric is similar to the one based on MD simulations [14]. Figure 9 shows that the neutron flux with energy above 0.5 MeV is not very representative of the attenuation of damage rates in RPVs as it in the SS heavy reflector shown in Ref. [5]. However, the neutron flux above 0.5 MeV is much more representative of damage rate than the total flux, the flux above 0.1 MeV, and the flux above 1 MeV for the attenuation in the RPVs. This conclusion is also verified by the data presented in Ref. [23] and shown in Figure 10: the ratio of DPA rates to neutron flux above 0.5 MeV in a RPV varies much less than the ratios to flux above 0, 0.1, and 1 MeV for a VVER-1000 (with standard and low leakage fuel loadings), German 1300 MW PWR, and German 900 MW BWR (the ratios of maximum to minimum shown in Figure 10 are respectively 2.7, 2.3, 1.3, and 2.3 for neutron flux above 0, 0.1, 0.5, and 1 MeV).

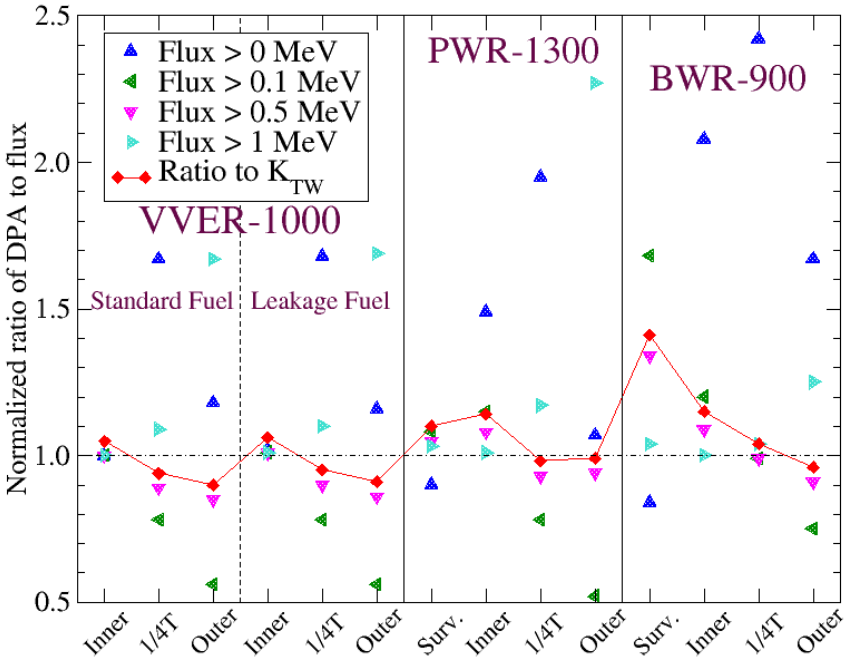

Figure 10. Normalized ratio of neutron-induced DPA to neutron flux above different threshold energies in RPVs for various reactors [23] and the ratio of K deduced from Ref. [23] to that obtained in this work (denoted by K_{TW}). The normalized ratios computed from Ref. [23] are normalized by the corresponding values for the inner surface of the VVER-1000 RPV with standard fuel loading (i.e. the left-most points in the figure). $K = \mathrm{DPA}/\phi_{>0.5}$ is defined in Eq. (11).

For comparison, Figure 9 also plots the attenuation formula proposed by the US NRC [8]:

$$DPA_n(x) = DPA_{n0}e^{-0.09449x}. \quad (10)$$

where x is in cm. Figure 9 shows that the US-NRC attenuation formula is globally consistent with the attenuations of DPA and neutron flux above 0.5 MeV in the RPVs of the presented PWR mock-ups. This formula is primarily proposed for fluence above 1 MeV [8], whereas the attenuation of neutron flux with energies above 1 MeV is faster than this formula. However, the US-NRC regulatory guide also mentions that the

attenuation of DPA may be substituted for the attenuation formula [8]. In this case, there is no large difference between the use of the US-NRC formula and the DPA calculations shown in the present work.

The NRC-proposed attenuation coefficient -0.09449/cm is quite close to the values determined in the present work: -0.09443/cm with a 22 cm thick heavy reflector and -0.10227/cm without a reflector. Especially for the case with a 22 cm SS heavy reflector, the difference is only 0.06% and Figure 9 shows quite good agreement between the damage rate and NRC's formula for penetration smaller than 17 cm. It is noteworthy that if Eq. (2) is applied, the absolute value of the attenuation coefficient is smaller. In the present study, the attenuation coefficients of Eq. (2) with and without the heavy reflector are respectively -0.07919/cm and -0.08728/cm. The absolute values of these two coefficients are larger than the ones determined in Ref. [3] (~ -0.07/cm for four PWRs).

Supposing the relationship between damage and neutron fluence above 0.5 MeV ($\phi_{>0.5}$) as:

$$\mathrm{DPA} = K\phi_{>0.5} \tag{11}$$

where K is the factor converting the neutron fluence ϕ with energies above 0.5 MeV (i.e. $\phi_{>0.5}$) into the searched DPA. It is deduced that $K \approx 9.5 \times 10^{-22}$ DPA/(n · cm^{-2}) in the RPV with and without a 22 cm thick heavy reflector. This value is slightly larger than $K = 8.6 \times 10^{-22}$ DPA/(n · cm^{-2}) for the heavy reflector [5] because the neutron flux in a RPV has a lower proportion of neutrons with energies above 0.5 MeV. It is noted that at the inner surface of the RPV in a 900 MWe French PWR of which the spectrum is given in Ref. [24], $K = 9.3 \times 10^{-22}$ DPA/(n · cm^{-2}) (based on JEFF-3.1.1). Figure 10 illustrates the ratios of K deduced from Ref. [23] to the coefficient $K \approx 9.5 \times 10^{-22}$ DPA/(n · cm^{-2}) obtained in the present work. It is observed that our value is quite close to the values for a VVER-1000 (with standard and low leakage fuel loadings), German 1300 MW PWR, and German 900 MW BWR (within [-10%, 15%] deviation except at surveillance position of the BWR), based on MCNP using ENDF/B-VI [23]. Therefore, the additional RPV in the PERLE benchmark is complementarily justified for studying the neutron-induced irradiation damage in PWR RPV. Moreover, Eq. (11) could provide an additional criterion on the representativity of neutron flux in RPV for experimental designs.

4. Conclusions

The present work investigates the attenuation of neutron and photon-induced irradiation damage in a PWR RPV. The studies are carried out on a simulated benchmark reproducing a Gen III-like UO_2 core surrounded by a SS thick reflector (issued from the PERLE experiment, conducted in the EOLE zero power reactor) with an additional RPV using Tripoli-4.10 Monte Carlo simulations. In order to evaluate the effect of different reflector thicknesses on irradiation damage, an extreme case that replaces the heavy reflector by a moderator is studied. In both cases, the photon-induced damage is well described by the exponential law with two free parameters (amplitude and attenuation coefficient). It is noteworthy that the photon-induced damage in PWR

RPV is about 100 times smaller than the neutron-induced one, whereas this factor is about 5000 in the SS heavy reflector [5].

For neutron-induced damage, the attenuation near the outer surface of a RPV is stronger than that predicted by exponential law due to the "leakage" of neutrons. The present work shows that the primary concrete has a positive contribution to the DPA in the RPV close to the outer surface by reflecting neutrons, whereas the contribution of the primary concrete and the enclosed air to DPA in the RPV is still less important than a SS. Regardless, the exponential law can be used to describe the attenuation of neutron-induced damage for penetration < 17 cm in a typical 22 cm RPV within 5% discrepancy. The exponential law with an additional negative term well fits the attenuation of neutron-induced damage in RPV. On the other hand, it is found that the presence of a SS heavy reflector reduces the neutron-induced damage in a RPV by a factor close to 2 (and > 2 if a smaller but more realistic distance between the core and RPV is considered).

Comparing the attenuation of neutron-induced damage and the neutron flux, it is verified that the neutron flux above 0.5 MeV is more representative of irradiation damage than the flux above 0, 0.1, and 1 MeV thresholds in RPV, while our previous work shows a similar conclusion in the SS heavy reflector [5]. The relationship $\mathrm{DPA} \approx K\phi_{>0.5}$ with $K = 9.5 \times 10^{-22}\ \mathrm{DPA}/(\mathrm{n}\cdot\mathrm{cm}^{-2})$ is determined in the RPVs for the two cases (i.e. with the heavy reflector and without a reflector). This coefficient is comparable with $K = 9.3 \times 10^{-22}\ \mathrm{DPA}/(\mathrm{n}\cdot\mathrm{cm}^{-2})$ at the inner surface of RPV of a French 900 MWe PWR. It is also coherent with the values at different depths of penetration in RPVs of a VVER-1000, a German 1300 MW PWR, and a German 900 MW BWR [23]. Moreover, the attenuation coefficients in the exponential form for neutron-induced damage determined in the present studies are close to the value proposed by the US NRC. However, it is notable that this value is larger than $K = 8.6 \times 10^{-22}\ \mathrm{DPA}/(\mathrm{n}\cdot\mathrm{cm}^{-2})$ [5] in the SS heavy reflector.

Appendix

Figure 11 shows the ratio of neutron spectra in the RPV illustrated in Figure 1(a) without the primary concrete nor the enclosed air to the reference case. It is used for comparison with Figure 2. Figure 12 (Figure 13 resp.) illustrates the attenuation of neutron and photon-induced damage rates with and without the heavy reflector in the case of no surrounded air/concrete (50 cm air + concrete resp.). These figures are for the sake of comparison with Figure 5 and Figure 6. Table 2 summarizes the goodness of fittings shown in Figure 12 and Figure 13.

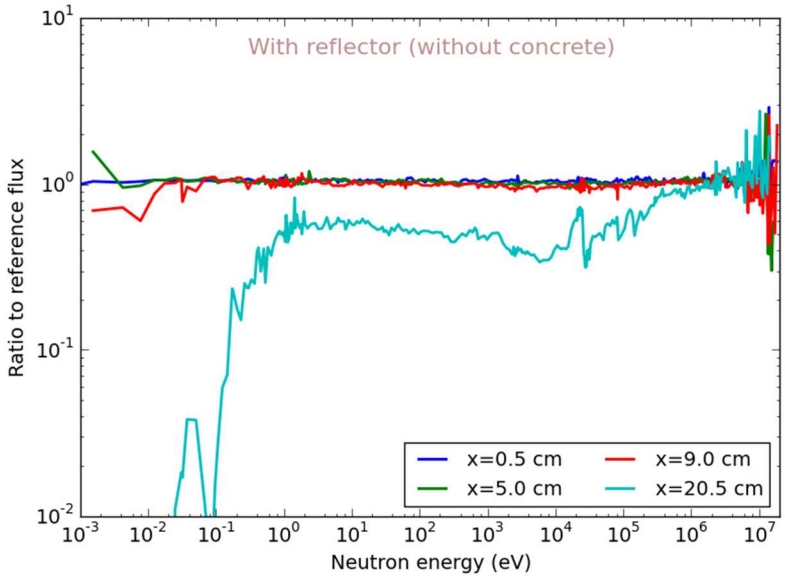

Figure 11. Ratio of neutron spectra at different penetrations in the RPV without the primary concrete nor the air between the RPV and the concrete to the reference case

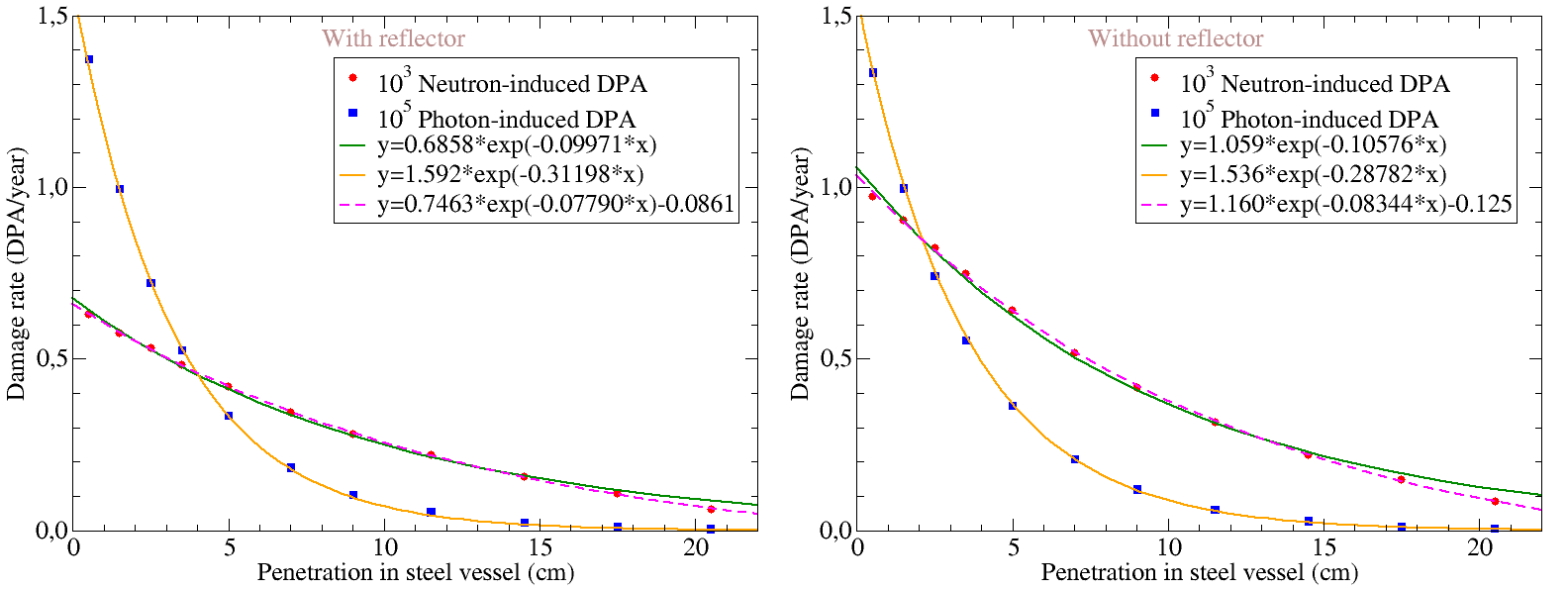

Figure 12. Attenuation of DPA rates in the RPV of the PERLE experiment with (left) and without (right) reflector without air/concrete enclosing the RPV

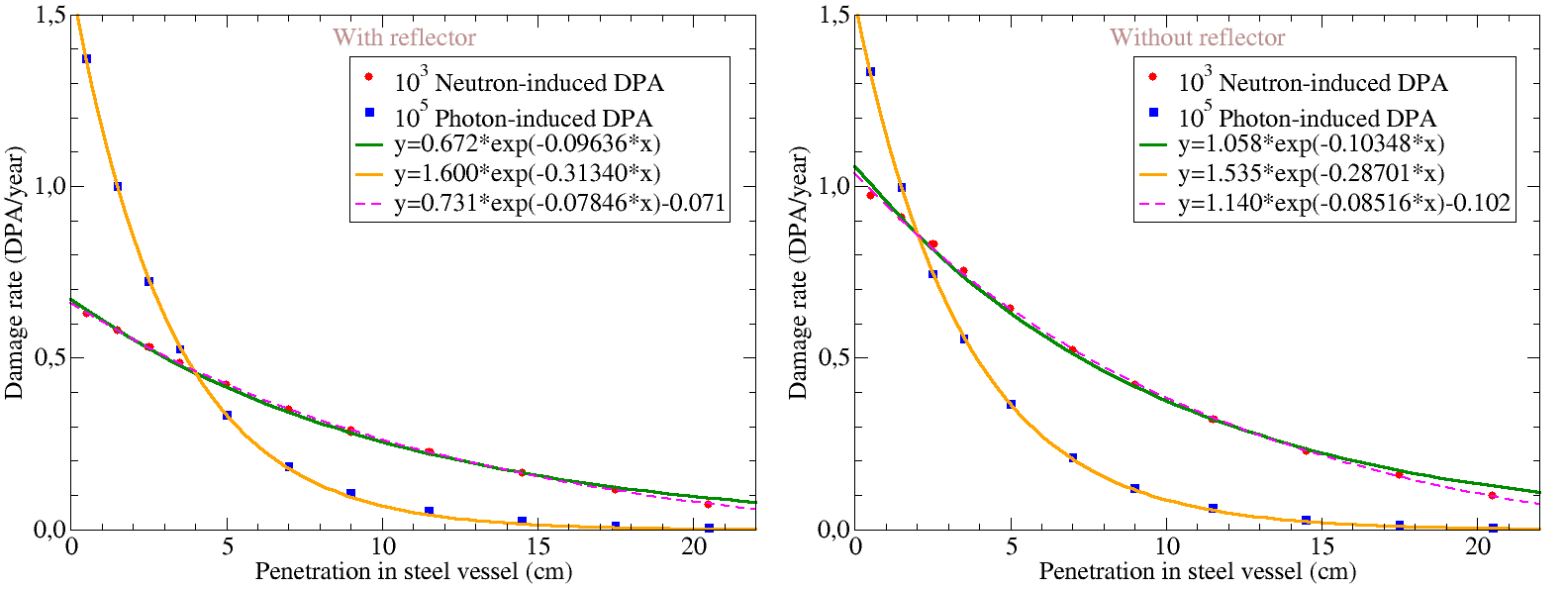

Figure 13. Attenuation of DPA rates in the RPV of the PERLE experiment with (upper) and without (lower) reflector with 50 cm air between the RPV and the concrete

Table 2. Goodness of non-linear curve fitting of the attenuation of damage rates shown in Figure 12 and Figure 13

Case		With reflector			Without reflector		
		Photon	Neutron (1)	Neutron (2)	Photon	Neutron (1)	Neutron (2)
Without	R^2	0.99990	0.99861	0.99994	0.99997	0.99842	0.99981
concrete	χ^2	0.01178	0.00263	0.00498	0.00488	0.00346	0.00038
50 cm air	R^2	0.99992	0.99904	0.99995	0.99997	0.99871	0.99966
+ concrete	χ^2	0.00050	0.00078	0.00004	0.00697	0.02572	0.01271

References

[1] R. Stoller and L. Greenwood, "An Evaluation of Through-Thickness Changes in Primary Damage Production in Commercial Reactor Pressure Vessels," in *Effects of Radiation on Materials: 20th International Symposium, ASTM STP 1405*, S. Rosinski, M. Grossbeck, T. Allen, and A. Kumar, Eds. American Society for Testing and Materials, West Conshohocken, PA, 2002.

[2] M. J. Norgett, M. T. Robinson, and I. M. Torrens, "A proposed method of calculating displacement dose rates," *Nucl. Eng. Des.*, vol. 33, no. 1, pp. 50–54, Aug. 1975, doi: 10.1016/0029-5493(75)90035-7.

[3] J. F. Carew and K. Hu, "Effect of Transverse Neutron Leakage on the Attenuation of the Displacements per Atom in the Reactor Pressure Vessel," *Nucl. Sci. Eng.*, vol. 152, no. 3, pp. 256–273, Mar. 2006, doi: 10.13182/NSE06-A2580.

[4] I. Remec, "Study of the Neutron Flux and Dpa Attenuation in the Reactor Pressure-Vessel Wall," Oak Ridge National Lab., TN (US), ORNL/NRC/LTR-99/5, Jun. 1999. doi: 10.2172/8343.

[5] S. Chen and D. Bernard, "Attenuation of atomic displacement damage in the heavy reflector of the PERLE experiment and application to EPR," *Nucl. Eng. Des.*, vol. 353, p. 110205, Nov. 2019, doi: 10.1016/j.nucengdes.2019.110205.

[6] E. Brun *et al.*, "TRIPOLI-4®, CEA, EDF and AREVA reference Monte Carlo code," *Ann. Nucl. Energy*, vol. 82, pp. 151–160, Aug. 2015, doi: 10.1016/j.anucene.2014.07.053.

[7] NEA, "Computing radiation dose to reactor pressure vessel and internals," State-of-the-Art Report NEA/NSC/DOC(96)5, 1996.

[8] Office of Nuclear Regulatory Research, "Radiation Embrittlement of Reactor Vessel Materials," U.S. Nuclear Regulatory Commission, Regulatory Guide 1.99, Rev. 2, May 1988. Accessed: Jun. 23, 2019. [Online]. Available: https://www.nrc.gov/docs/ML0037/ML003740284.pdf.

[9] G. Sengler, F. Forêt, G. Schlosser, R. Lisdat, and S. Stelletta, "EPR core design," *Nucl. Eng. Des.*, vol. 187, no. 1, pp. 79–119, Jan. 1999, doi: 10.1016/S0029-5493(98)00259-3.

[10] A. Santamarina *et al.*, "The PERLE experiment for the qualification of PWR heavy reflectors," in *Proc. of Int. Conf. on the Physics of Reactors: Nuclear Power: A Sustainable Resource (PHYSOR2008)*, Interlaken, Switzerland, Sep. 2008.

[11] C. Vaglio-Gaudard *et al.*, "Interpretation of PERLE Experiment for the Validation of Iron Nuclear Data Using Monte Carlo Calculations," *Nucl. Sci. Eng.*, vol. 166, no. 2, pp. 89–106, Oct. 2010, doi: 10.13182/NSE09-91.

[12] A. Santamarina *et al.*, "The JEFF-3.1.1 Nuclear Data Library," OECD/NEA, JEFF Report 22, NEA No. 6807, 2009.

[13] S. Ravaux, "Qualification du Calcul de l'Échauffement Photonique dans les Réacteurs Nucléaires," Université de Grenoble, 2013.

[14] R. E. Stoller, "Evaluation of neutron energy spectrum effects and RPV thru-wall attenuation based on molecular dynamics cascade simulations," *Nucl. Eng. Des.*, vol. 195, no. 2, pp. 129–136, Feb. 2000, doi: 10.1016/S0029-5493(99)00241-1.

[15] Y. Peneliau, "Electron Photon Shower Simulation in TRIPOLI-4 Monte Carlo Code," in *Advanced Monte Carlo for Radiation Physics, Particle Transport Simulation and Applications*, Berlin, Heidelberg, 2001, pp. 129–134, doi: 10.1007/978-3-642-18211-2_22.

[16] S. Chen, D. Bernard, and C. De Saint Jean, "Calculation and analysis of gamma-induced irradiation damage cross section," *Nucl. Instrum. Methods Phys. Res. Sect. B Beam Interact. Mater. At.*, vol. 447, pp. 8–21, May 2019, doi: 10.1016/j.nimb.2019.03.035.

[17] S. Chen, D. Bernard, and L. Buiron, "Study on the self-shielding and temperature influences on the neutron irradiation damage calculations in reactors," *Nucl. Eng. Des.*, vol. 346, pp. 85–96, May 2019, doi: 10.1016/j.nucengdes.2019.03.006.

[18] R. E. MacFarlane, D. W. Muir, R. M. Boicourt, A. C. Kahler, and J. L. Conlin, "The NJOY Nuclear Data Processing System, Version 2016," Los Alamos National Laboratory (LANL), Los Alamos, NM, United States, LA-UR-17-20093, 2016.

[19] D. E. Alexander and L. E. Rehn, "The contribution of high energy gamma rays to

displacement damage in LWR pressure vessels," *J. Nucl. Mater.*, vol. 209, no. 2, pp. 212–214, Apr. 1994, doi: 10.1016/0022-3115(94)90297-6.

[20] D. E. Alexander and L. E. Rehn, "Gamma-ray displacement damage in the pressure vessel of the advanced boiling water reactor," *J. Nucl. Mater.*, vol. 217, no. 1, pp. 213–216, Nov. 1994, doi: 10.1016/0022-3115(94)90325-5.

[21] I. Remec, J. A. Wang, F. B. K. Kam, and K. Farrell, "Effects of gamma-induced displacements on HFIR pressure vessel materials," *J. Nucl. Mater.*, vol. 217, no. 3, pp. 258–268, Dec. 1994, doi: 10.1016/0022-3115(94)90375-1.

[22] C. P. Keegan, J. H. Scobel, and R. F. Wright, "Nuclear reactor vessel fuel thermal insulating barrier," US8401142B2, Mar. 19, 2013.

[23] B. Boehmer *et al.*, "Neutron and gamma fluence and radiation damage parameters of ex-core components of Russian and German light water reactors," presented at the Reactor Dosimetry in the 21st Century, Jun. 2003, pp. 286–294, doi: 10.1142/9789812705563_0036.

[24] S. Chen *et al.*, "Calculation and verification of neutron irradiation damage with differential cross sections," *Nucl. Instrum. Methods Phys. Res. Sect. B Beam Interact. Mater. At.*, vol. 456, pp. 120–132, Oct. 2019, doi: 10.1016/j.nimb.2019.07.011.